

Patterned PLG substrates for localized DNA delivery and directed neurite extension

Tiffany Houchin-Ray^{a,1}, Laura A. Swift^{a,1}, Jae-Hyung Jang^d, Lonnie D. Shea^{a,b,c,*}

^aDepartment of Chemical and Biological Engineering, Northwestern University, 2145 Sheridan Rd./E156, Evanston, IL 60208-3120, USA

^bDepartment of Biomedical Engineering, Northwestern University, 2145 Sheridan Rd./E156, Evanston, IL 60208-3120, USA

^cDepartment of Institute for BioNanotechnology in Medicine, 2145 Sheridan Rd./E156 Evanston, IL 60208-3120, USA

^dDepartment of Chemical Engineering and the Helen Wills Neuroscience Institute, University of California at Berkeley, Berkeley, CA, USA

Received 11 October 2006; accepted 23 January 2007

Available online 9 February 2007

Abstract

Tissue engineering strategies that enable nerve regeneration will require methods that can promote and direct neurite extension across the lesion. In this report, we investigate an *in vitro* combinatorial approach to directed neurite outgrowth using gene delivery from topographically patterned substrates, which can induce expression of neurotrophic factors to promote neurite extension and direct the extending neurites. Poly(lactide-*co*-glycolide) (PLG), which has been used to fabricate conduits or bridges for regeneration, was compression molded to create channels with 100, 150, and 250 µm widths. DNA complexes were immobilized to the PLG, and cells cultured on the substrate were transfected with efficiencies dependent on channel width and DNA amount. A co-culture model consisting of primary neurons and accessory cells was employed to investigate neurite outgrowth within the channels. Localized secretion of nerve growth factor (NGF) by the accessory cells promoted neuron survival and neurite extension. Neurons cultured in channels with NGF expression exhibited longer primary neurites than in the absence of channels. Neurons cultured in smaller width PLG microchannels exhibited a greater degree of directionality and less secondary sprouting than larger channels. Finally, surface immobilization allowed for the delivery of distinct plasmids from each channel, which may enable channels to be tailored for specific nerve tracts. This approach demonstrates the ability to combine gene delivery with physical guidance, and can be tailored to target specific axonal populations with varying neurotrophic factor requirements.

© 2007 Elsevier Ltd. All rights reserved.

Keywords: Gene delivery; Substrate-mediated delivery; Nerve guidance; PLG; Nerve regeneration

1. Introduction

Injury to a nerve results in paralysis below the lesion, and nerve regeneration across the lesion is a first step towards regaining function. In the spinal cord, neurons have the potential to regenerate, but growth is limited by the extracellular environment [1–3]. An approach to manipulate the local environment involves the implantation of biomaterial scaffolds that are termed bridges.

Bridges implanted at the lesion function to maintain a continuous path for regeneration, promote infiltration of permissive cell types that can secrete inductive factors, support axonal elongation, and reduce scar formation [4,5]. Recently, bridges have been engineered with channels that may function to physically guide extending neurites and segregate functional pathways [6–9]. The physical boundaries provided by the channels can produce longer and oriented neurites, which may otherwise be random [8]. While bridges support axonal growth, the density of axons remains significantly less than native tissue (for review, see [5]).

Neurotrophic factors, such as nerve growth factor (NGF), neurotrophin-3 (NT-3), and brain-derived neurotrophic factor (BDNF), delivered at a lesion can enhance

*Corresponding author. Department of Chemical and Biological Engineering, Northwestern University, 2145 Sheridan Rd./E156, Evanston, IL 60208-3120, USA. Tel.: +1 847 491 7043; fax: 847 491 3728.

E-mail address: l-shea@northwestern.edu (L.D. Shea).

¹Authors have contributed equally to this manuscript.

the density of axons growing through the lesion [10,11]. Injured neurons remain responsive to the neurotrophins, yet the local concentration produced endogenously is insufficient to promote regeneration [12]. Delivering these factors can act directly on the neurons to promote survival and axonal elongation. Neurotrophic factors have been delivered via protein injection and the transplantation of ex vivo engineered cells [13]. These methods of protein delivery are met by limitations, such as clearance, degradation, and instability, and do not maintain therapeutic concentrations of neurotrophic factors for sustained periods of time. More recently, bridges capable of controlled release have been developed with the potential to provide a more controlled and localized dose relative to traditional delivery methods [6,13].

Gene delivery is a versatile alternative to direct protein delivery, with the potential for delivery from biomaterials to provide localized inductive expression of proteins for extended times [14]. An approach to delivering DNA from a tissue engineering scaffold involves immobilization of the vector to the scaffold, a process termed substrate-mediated delivery [15]. DNA is complexed with a cationic lipid or polymer for immobilization by specific and/or non-specific interactions between the vector and substrate [16,17]. Substrate-mediated delivery places DNA at or near the biomaterial surface, which can promote internalization by those cells adhering to the scaffold [18]. This delivery approach enables scaffolds to be fabricated by any technique and in any geometry for subsequent immobilization without affecting the DNA stability. Additionally, immobilization provides a means to spatially localize gene transfer, which may be useful for recreating the architecture of complex tissues.

In this report, the delivery of genes encoding for neurotrophic factors was combined with physical guidance barriers to promote neuron survival and neurite outgrowth and simultaneously direct extending neurites in vitro. Two-dimensional poly(lactide-*co*-glycolide) (PLG) scaffolds with topographical patterns were fabricated via compression molding on poly(dimethylsiloxane) (PDMS) templates. PLG has been widely used as bridges for spinal cord repair, or conduits for peripheral nerve regeneration [4]. Non-viral DNA complexes were created by mixing plasmid DNA with a cationic polymer, polyethylenimine (PEI). These non-viral DNA complexes were immobilized to the PLG surface and both transfection efficiency and transgene expression were investigated as a function of channel width and DNA amount. DNA encoding NGF was subsequently non-specifically immobilized to the PLG microchannels and an in vitro co-culture model was employed to assess neuron survival and neurite extension [19]. Additionally, the ability to localize gene transfer to the channel in order to tailor channels for specific axonal populations was investigated. This study identifies design parameters for applying the delivery mechanism to three-dimensional (3D) structures for the promotion of nerve regeneration.

2. Materials and methods

2.1. Fabrication of flat PLG disks

PLG (75:25 mole ratio of D,L-lactide to glycolide *i.v.* = 0.6–0.8) (Boehringer Ingelheim Chemical, Petersburg, VA) pellets were heated to 82 °C and pressed into a flat disk using a 5 kg weight. The temperature was slowly decreased from 82 to 37 °C and the disks were placed at 37 °C overnight. Disks had a radius of approximately 1.55 cm and were stored at room temperature until use.

2.2. Fabrication of patterned PLG disks

Templates containing the desired pattern were constructed using photolithography. SU8-100 negative-tone photoresist (Microchem, Newton, MA) was spin coated at 1000 rpm for 30 s on silicon wafers (Ultrasil, Hayward, CA). After baking, specific regions of the photoresist were polymerized using film transparencies as the photomask (In Tandem Design, Towson, MD) and a Quintel Q-2000 mask aligner (Quintel, San Jose, CA), with UV exposure for 45 s. The photoresist was patterned with raised lines that were 250 μm wide, 150 μm high, and 10 mm long. The distance between the lines varied in the following order: 100, 150, and 250 μm, and this distance between the lines determined the channel width. A second pattern was fabricated to achieve uniform channels on a single disk. In this case, the distance between the lines was held constant at either 100, 150, or 250 μm. PDMS (Krayden, Glenview, IL), also referred to as Dow Corning Sylgard 184 Elastomer, was cured on the photoresist molds at a 10:1 (base to curing agent) ratio at 60 °C for 5 h. After cooling, the PDMS was peeled from the silicon wafer, leaving a template of the fabricated pattern. To fabricate patterned PLG disks, the PDMS template was coated with PLG pellets, heated, and the polymer was molded as described in Section 2.1. Patterned disks were stored at room temperature until use.

2.3. DNA complex immobilization

Prior to complex immobilization, PLG disks (flat and patterned) were attached to the bottom of wells of a 24-well tissue culture plate with autoclaved silicon grease. Disks were incubated with 50% fetal bovine serum (FBS) in phosphate-buffered saline (PBS) for 4 h at room temperature. Plasmid was complexed with PEI (25 kDa, Aldrich, St. Louis, MO) in a total volume of 300 μL to form PEI/DNA complexes at three fixed DNA amounts: 1, 3, and 6 μg by dropwise addition of PEI to plasmid and subsequent mixing. The amount of PEI was varied to achieve an N/P ratio of 25 while both DNA and PEI were diluted with 150 mM NaCl. Complexes were incubated at room temperature for 10 min, and then incubated on the PLG disks at room temperature for 1 h. For gene delivery within each channel, the complexes (\approx 10 μL) were deposited into individual channels using a mouth pipette. The complexes quickly adsorbed to the PLG, therefore, multiple depositions ($n = 5$) were performed sequentially. For imaging deposition, plasmid (pEGFP-Luc) was fluorescently labeled with tetramethyl rhodamine using the manufacturer's protocol (Mirus, Madison, WI). The deposited DNA was imaged with fluorescence microscopy (Leica) and complex size was measured using the NIH program *Image J* (available at <http://rsb.info.nih.gov/nih-image>).

2.4. Cell culture and transfection

Transfection studies were performed with HEK293T cells (ATCC, Manassas, VA) cultured at 5% CO₂ and 37 °C in Dulbecco's Modified Eagle Medium (DMEM) supplemented with 10% heat-inactivated FBS, 1% penicillin-streptomycin, and 1% sodium pyruvate (cDMEM). Cells were seeded at a density of 100,000 cells per PLG disk (flat and patterned). For substrate-mediated delivery, cells were seeded directly following

complex immobilization. Transfection was analyzed following a 48 h culture.

Transfection was characterized through the extent of transgene expression (luciferase levels) and the number of transfected cells (β -galactosidase expression). The dual reporter plasmid pEGFPLuc (Clontech, Mountain View, CA), which contains both EGFP and luciferase driven by a CMV promoter, was used to determine the extent of transgene expression. Luciferase transgene levels were measured using the Luciferase Assay System (Promega, Madison, WI). After 48 h in culture, cells were lysed and assayed using a luminometer (Turner Biosystems) set for a 3-s delay with signal integration for 10 s. Luciferase activity was normalized to the total amount of protein. To assess luciferase activity within individual sized channels, pEGFPLuc complexes were immobilized to disks with uniform sized channels. Before cell lysis, the cells cultured on top of the channels were removed by scraping, as to achieve an accurate quantification of expression by cells cultured within the channels. The reporter plasmid β -galactosidase (pNGVL1-nt-LacZ) (National Gene Vector Labs, Ann Arbor, MI) was used to determine the number of transfected cells. Expression was visualized using X-gal stain, and the total number of transfected cells was counted from five random pictures of the PLG surface. The total number of cells within each image was determined by staining with 5 μ g/mL Hoechst 33258 (Molecular Probes, Eugene, OR) and counting the cells using cell counting software, CellC version 1.11 (available at <http://www.cs.tut.fi/sgn/csb/cellc/>).

2.5. In vitro neurite outgrowth

The plasmid encoding for NGF (pNGF) has full-length mouse NGF in the RK5 vector backbone with a CMV promoter, and was a gift from Dr. Hiroshi Nomoto (Gifu Pharmaceutical University, Japan). pNGF was complexed with PEI (N/P = 25) and immobilized to the PLG substrates as described in Section 2.3. Following two PBS rinses, HEK293T cells were cultured on the PLG substrates. To obtain primary neurons, dorsal root ganglia (DRG) were isolated from E8 white leghorn chicken embryos (Michigan State University Poultry Center, East Lansing, MI) and maintained in Hank's balanced salt solution (HBSS) buffer supplemented with 6 g/L glucose until the isolation was complete. DRG were incubated for 30 min at 37 °C in 0.25% trypsin (Worthington Biochemical, Lakewood, NJ), followed by trituration with fire-polished glass Pasteur pipettes to dissociate the ganglia. Non-neuronal and neuronal cells were separated by panning for 2 h at 37 °C. After 8 h culture of the HEK293T cells, the media was removed, the surfaces were washed with PBS, and dissociated DRG neurons were seeded (5×10^4 cells/well) on the cell layer. Control conditions included DRG neurons co-cultured with HEK293T cells with no DNA deposited and various concentrations of recombinant rat β -NGF (R&D Systems, Minneapolis, MN) (0.1, 1.0, 10, and 25 ng/mL) added to the culture media at the time of DRG seeding. Cells were co-cultured for 48 h in cDMEM at 37 °C, 5% CO₂ and fixed with 4% paraformaldehyde (PFA) after the culture period. The neurons were stained for neuron-specific class III β -tubulin by incubating fixed cells in TUJ1 antibody (Covance, Berkely, CA) diluted in 5% normal goat serum (Vector Labs, Burlingame, CA) in PBS for 1 h followed by incubation in TRITC-conjugated goat anti-mouse secondary antibody (Jackson ImmunoResearch, West Grove, PA) in PBS for 30 min. Cells were counter-stained with Hoechst 33258 to visualize cell nuclei. Neurons and HEK293Ts were visualized with confocal microscopy (Leica Laser Confocal Microscope).

2.6. Neuron survival and neurite length quantification

Surviving neurons were identified as having sprouting neurites. Primary and secondary neurite length were measured using *Image J* with a Neuron J plug-in [20]. Primary neurites were defined as extending directly from the neuron cell soma. Secondary neurites were defined as extending from a primary neurite. Quantifications were made from five regions of each disk or channel size and averaged.

2.7. Statistics

Statistical analysis was performed using JMP software (SAS Institute, Cary, NC). Comparative analyses were executed using one-way ANOVA with Tukey post-tests, at a 95% confidence level. Mean values with standard error of the mean (SEM) are reported. All experiments were performed in triplicate.

3. Results

3.1. Cellular transfection on PLG substrates

Initial studies evaluated the transfection efficiency and transgene expression with polyplexes non-specifically immobilized to compression molded, flat PLG disks. Three DNA amounts (1, 3, and 6 μ g) were incubated on the substrate for immobilization, with approximately 3% of the DNA remaining immobilized to the surface after washing [18]. Transfected cells were homogeneously distributed across the PLG disks (Fig. 1a). Transfection efficiency (percent of transfected cells) by immobilized polyplexes on PLG increased with increasing DNA amounts on the surfaces (Fig. 1b, $p < 0.05$). Efficiency ($33 \pm 2\%$) was maximal with 6 μ g DNA incubated on PLG surfaces. Protein expression on PLG disks increased from 1.3×10^5 to 7.1×10^6 RLU/mg protein, when the DNA amount incubated on the surface increased from 1 to 6 μ g (Fig. 1c, $p < 0.05$).

3.2. Complex immobilization and cellular transfection on patterned PLG

PLG disks with topographical patterns were capable of DNA immobilization and subsequent surface transfection depending on channel width. Each patterned PLG disk contained a double pattern of 100, 150, and 250 μ m channels (Fig. 2a) or six uniform sized channels (Fig. 2b), spaced by 250 μ m wide and 150 μ m high walls. Complexes deposited on the PLG substrate were homogeneously distributed independent of the channel width. The number of complexes with a diameter greater than 2 μ m within the 100 and 150 μ m channels was significantly increased relative to either the flat PLG disks or the 250 μ m channels, suggesting that complexes may have aggregated in the smaller channels (Fig. 2c–f). Cellular transfection within all sized channels (100, 150, and 250 μ m) was achieved by immobilization of DNA complexes (Fig. 3a–c). For incubation of 3 μ g DNA on the surface, transfection efficiency within all channel sizes (~5%) was less than on flat PLG disks (~15%) (Fig. 3d, $p < 0.05$). A significant increase in transfection efficiency was observed in all channel widths when the DNA amount was increased from 3 to 6 μ g (Fig. 3d, $p < 0.05$), similar to the result shown with flat PLG disks. For 6 μ g DNA incubated, transfection efficiency increased to ($16 \pm 2\%$) in the 100 μ m channel and ($30 \pm 2\%$) in the 150 μ m channel (Fig. 3d). Additionally, transfection efficiency in the 250 μ m channel ($52 \pm 7\%$) was

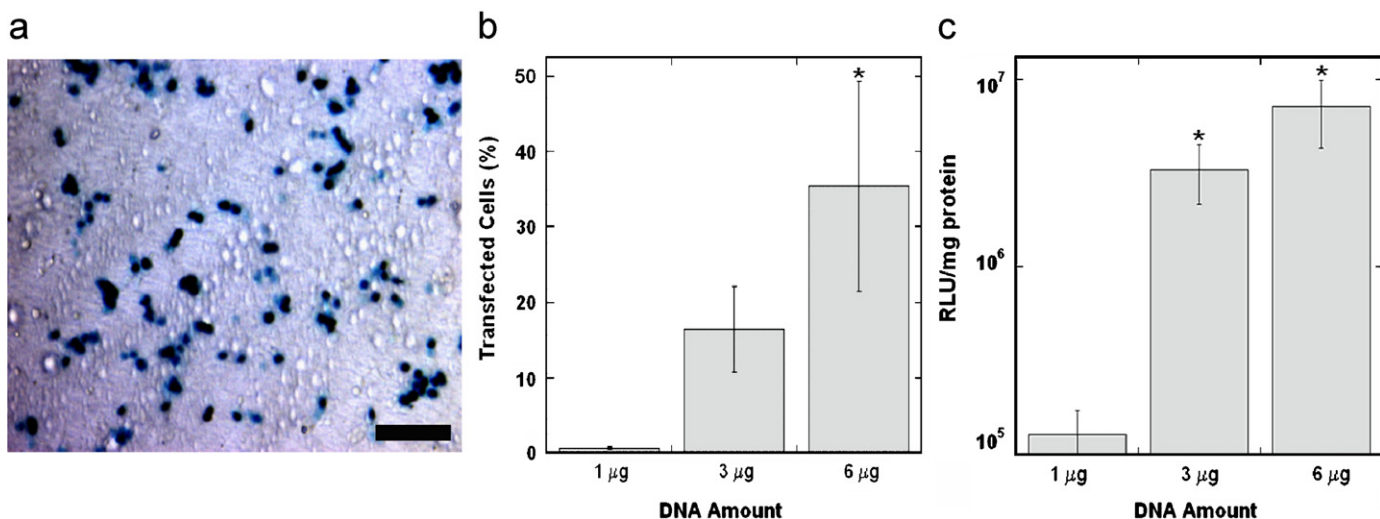


Fig. 1. Cellular transfection on flat PLG disks. X-gal staining of transfected HEK293T cells on a transparent PLG disk (a). Scale bar represents 100 μm. Comparison of transfection efficiency (b) and transgene expression (c) on PLG disks with varying DNA amounts. The symbol * indicates statistical significance, $p < 0.05$.

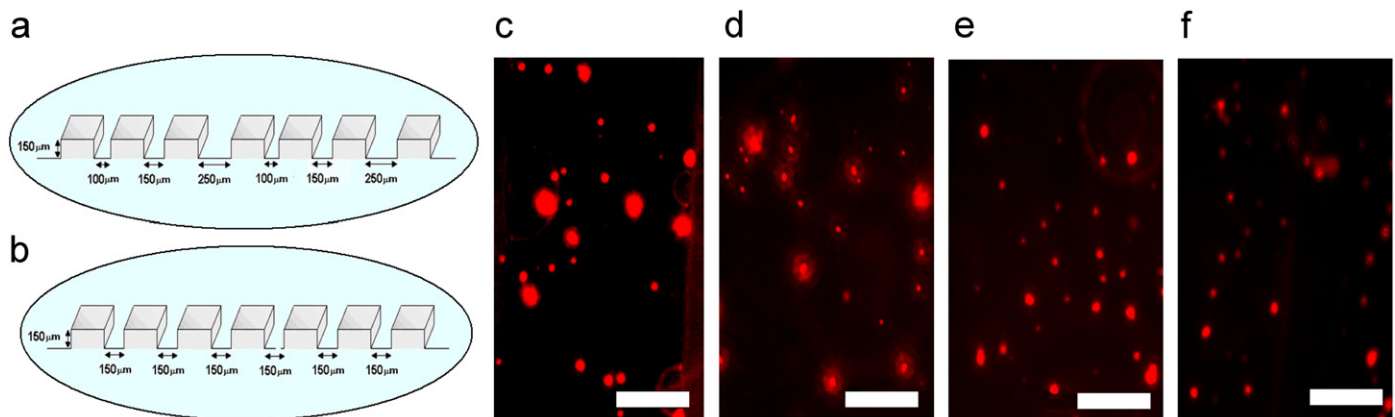


Fig. 2. DNA complex deposition within PLG microchannels. Schematic of patterned PLG disks fabricated by compression molding (a, b). Fluorescently labeled DNA complexes within 100 μm (c), 150 μm (d), and 250 μm (e) channels and on flat PLG disks (f). Scale bars represent 100 μm.

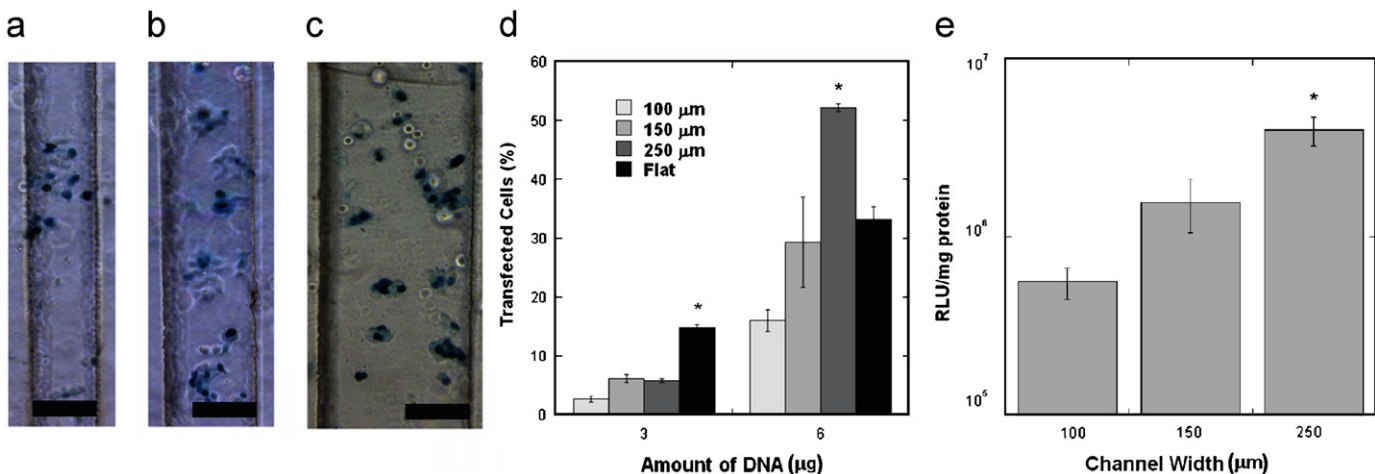


Fig. 3. Cellular transfection within PLG microchannels. X-gal staining of transfected HEK293T cells within 100 μm (a), 150 μm (b), and 250 μm (c) channels. Scale bars represent 100 μm. Comparison of transfection efficiency (d) and transgene expression (e) within the different width channels. The symbol * indicates statistical significance, $p < 0.05$.

significantly higher than efficiency in the smaller channels (Fig. 3d, $p<0.05$). For 6 µg DNA incubated, protein expression also increased with channel width from 5.6×10^5 RLU/mg protein (100 µm channel) to 4.0×10^6 RLU/mg protein (250 µm channel) (Fig. 3e, $p<0.05$).

3.3. Neuronal co-culture on flat PLG substrates

Primary neurons were co-cultured with HEK293T cells on flat PLG disks and assessed for neuron survival and neurite extension. pNGF (6 µg) was incubated on the PLG surface, the condition that yielded the highest percent transfected cells and protein expression level (Fig. 1). Significant neuron survival and neurite extension was present on surfaces with pNGF/PEI complexes deposited (Fig. 4a), but not on surfaces with either pLUC/PEI complexes (Fig. 4b), or in the absence of a vector (Fig. 4c). HEK293T cells were chosen for the co-culture model as they do not basally support neuron survival and neurite extension (Fig. 4c); thus, the neuronal response resulted from the production and secretion of NGF by the HEK293T cells. Neuron survival on pNGF/PLG disks ($35.6 \pm 5.2\%$) was higher than on disks with no DNA ($2.0 \pm 0.9\%$) or disks with immobilized pLUC/PEI complexes ($1.7 \pm 1.1\%$) (Fig. 4d, $p<0.001$). Furthermore, neuron survival on pNGF-PLG disks was comparable to survival on disks with 25 ng/mL NGF added to the cell culture media (Fig. 4d). In addition to neuron survival, total neurite extension per surface area was higher on pNGF-PLG disks ($81.4 \pm 7.2 \text{ cm}^{-1}$), compared to disks with no DNA ($1.9 \pm 0.9 \text{ cm}^{-1}$) or pLUC-PLG disks ($1.7 \pm 0.8 \text{ cm}^{-1}$), and comparable to PLG disks with 25 ng/mL NGF ($72.3 \pm 8.4 \text{ cm}^{-1}$) (Fig. 4e, $p<0.001$). The distribution of primary and secondary neurite density was subsequently investigated. Primary neurites extend directly from the neuron cell soma, while secondary neurites branch from primary neurites. Primary and secondary neurite

densities were quantified by measuring the total length of primary and secondary neurites and normalizing to the surface area. The primary neurite density on flat PLG disks with pNGF transfected cells was $26.5 \pm 3.2 \text{ cm}^{-1}$, while the secondary neurite density was $24.3 \pm 3.6 \text{ cm}^{-1}$.

3.4. Neuronal co-culture on patterned PLG

The ability to direct neurite extension was assessed by co-culturing primary neurons and HEK293T cells in the PLG channels, with 6 µg pNGF incubated. Neurons attached to the surface and sprouted neurites in channels of all sizes (Fig. 5a–d). Additionally, neurites in the 100 µm channel have neurites that contact and extend parallel to the channel wall (Fig. 5a), suggesting guidance by the wall. The larger channel widths display greater branching, with less neurites growing along the channel wall (Fig. 5b, c). Interestingly, neurites that did not contact the channel wall in the 100 µm channels also exhibited less branching than those in the 250 µm channels. The primary neurite density in the 100 µm channel ($89.2 \pm 11.2 \text{ cm}^{-1}$) was significantly greater than all other conditions (Fig. 5e, $p<0.05$). The primary neurite densities in the 150 µm ($60.2 \pm 2.2 \text{ cm}^{-1}$) and 250 µm ($47.3 \pm 4.1 \text{ cm}^{-1}$) channels were significantly greater than that on the flat PLG disk ($26.5 \pm 3.2 \text{ cm}^{-1}$) (Fig. 5e, $p<0.05$). Additionally, the ratio of primary to secondary neurite density decreased (from 2.3 to 1.2) as the channel size increased (from 100 to 250 µm).

To evaluate whether the differences in primary neurite outgrowth between different width channels could be attributed to variations in NGF concentration, neurons were cultured in the channels and NGF was added to the cell culture media to a final concentration ranging between 0.1 and 25 ng/mL. For a given channel width, the primary neurite density and degree of secondary sprouting did not change with varying NGF concentrations (Fig. 5f). Primary neurite density was significantly greater in the

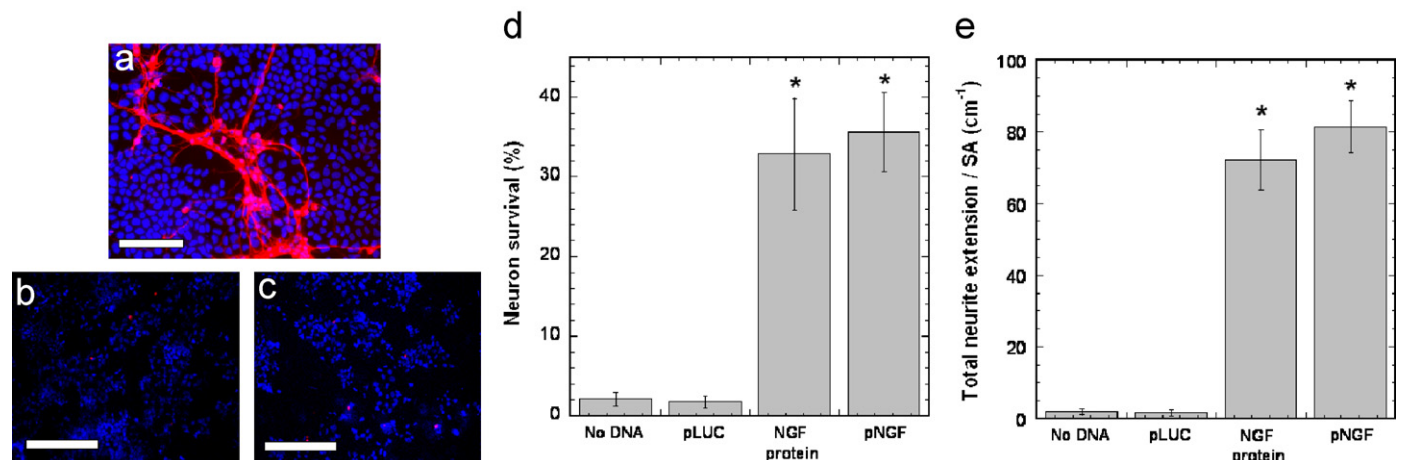


Fig. 4. Neuronal co-cultures on flat PLG disks. Neurite extension on PLG disks with: surface immobilized pNGF/PEI complexes (a), surface immobilized pLUC/PEI complexes (b), and no DNA (c). TUJ1 (red) and Hoechst 33258 nuclear stain (blue) images shown are overlaid. Scale bars represent 100 µm. Quantification of neuron survival (d) and total neurite extension normalized to surface area (e) on pNGF-PLG disks and control disks. The symbol * indicates statistical significance, $p<0.001$.

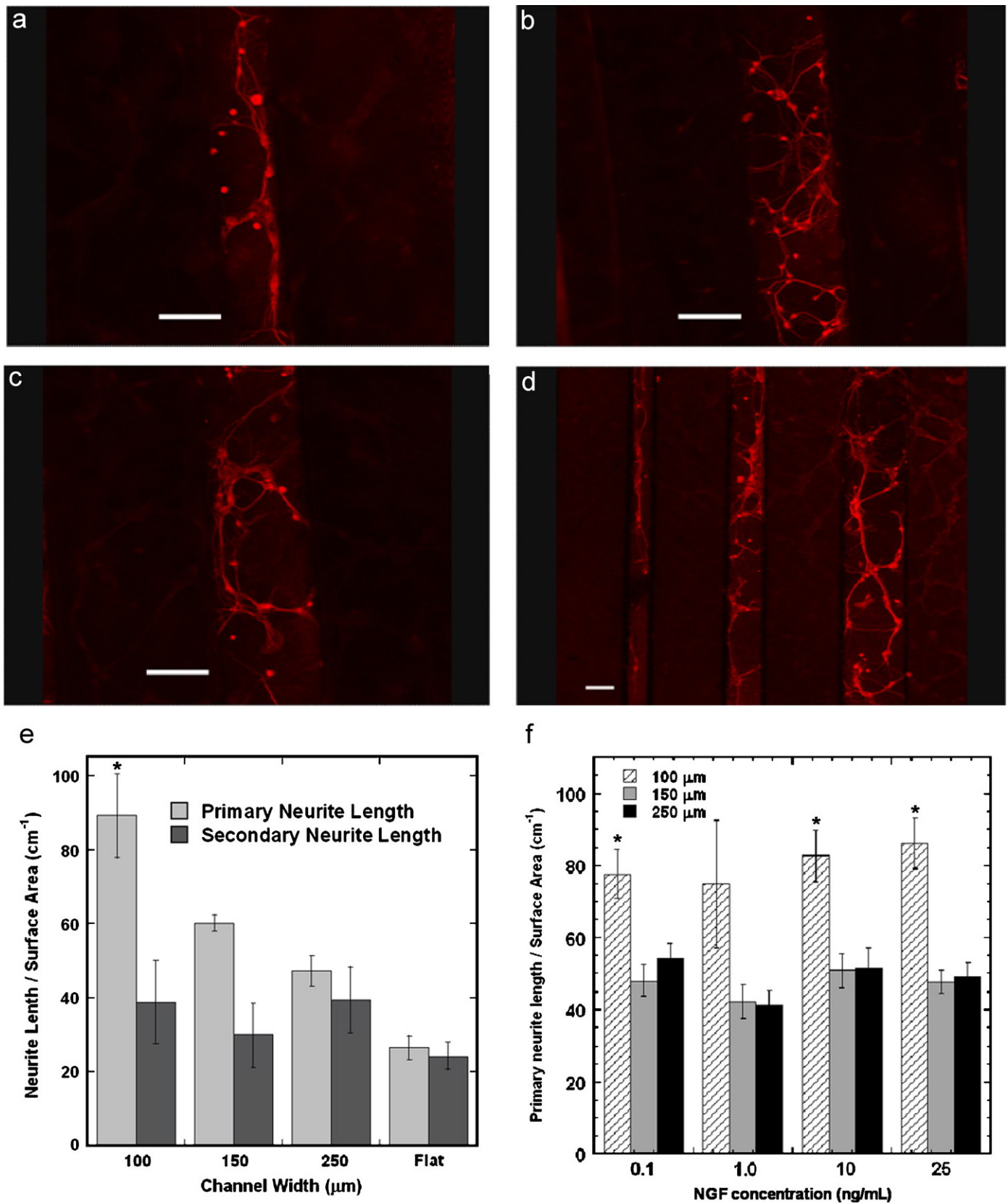


Fig. 5. Neuronal co-cultures within PLG microchannels. Fluorescence imaging of neurons cultured within PLG channels with immobilized pNGF/PEI complexes: 100 μm (a), 150 μm (b), 250 μm (c), and all channel widths (d). Scale bars represent 100 μm. Length of primary and secondary neurites per surface area within the PLG channels and on flat PLG disks with immobilized pNGF/PEI complexes (e). Length of primary neurites per surface area within PLG channels with various NGF concentrations added to the culture media (f). The symbol * indicates statistical significance, $p < 0.05$.

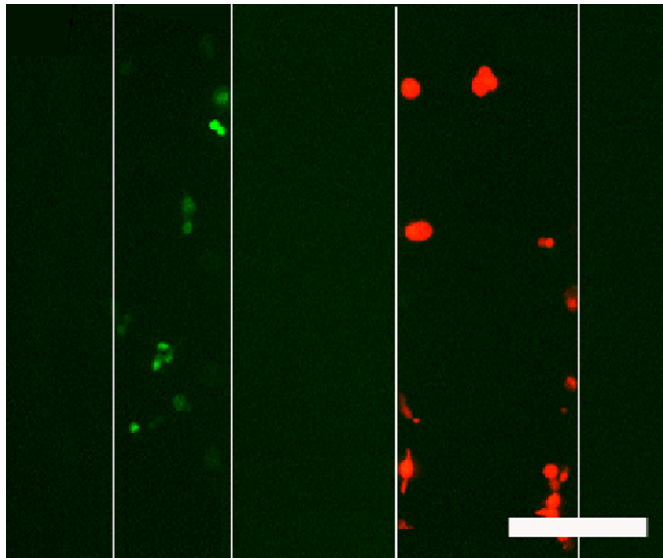


Fig. 6. Localized transfection in PLG channels. Complexes encoding for EGFP or DsRed were deposited into separate PLG channels. DsRed (red) and EGFP (green) images are overlaid. Scale bar represents 100 μ m.

100 μ m channels as compared to the 250 μ m channels for each NGF concentration (Fig. 5f, $p < 0.05$). Interestingly, the ratio of primary neurite density in the 100 versus 250 μ m channel was greater when neurons were co-cultured with pNGF transfected cells (1.9) as compared to neurons with NGF added to the media (1.45).

3.5. Patterned cellular transfection in PLG channels

Subsequent studies investigated the ability of substrate-mediated delivery to transfect cells only within the channel, and to enable transfection with different plasmids within each channel. Techniques were developed to isolate DNA/PEI complexes encoding for different plasmids within each channel of the patterned PLG disk. DNA/PEI complexes encoding for DsRed (pDsRed/PEI) and EGFP (pEGFP/PEI) were pipetted individually into separate PLG channels. This deposition procedure maintained the activity of the complexes, as transfected cells were observed within the channels. Importantly, cells cultured in the channel with immobilized pDsRed expressed DsRed efficiently with no visual evidence of EGFP expression. Similarly, channels with immobilized pEGFP did not exhibit cellular expression of DsRed (Fig. 6).

4. Discussion

Bridges for nerve regeneration must provide signals that promote neuron survival and neurite extension, while simultaneously directing regenerating neurites across the injury. Bridges that provide neurotrophic factors at therapeutic concentrations while providing guidance could enable novel approaches for regeneration. This report demonstrates the ability to immobilize DNA complexes within PLG channels for localized secretion of

neurotrophic factors. PLG was fabricated with channels of widths ranging from 100 to 250 μ m. The dimensions of the channels mimic the channels within 3D PLG scaffolds fabricated for in vivo spinal cord implantation [6]. Non-specifically adsorbed complexes yielded efficient transfection within the channels, with efficiencies comparable to that on flat PLG disks, with transfection dependent upon the channel width and DNA amount. NGF secreted by the transfected cells supported neuron survival and neurite extension, and the size of the channel influenced the ability of the guidance channels to direct neurite extension.

The width of the channels influenced transfection efficiency and protein expression by cells cultured on the substrates. For incubation with 6 μ g DNA, transfection efficiency and transgene expression in 100 μ m channels were significantly lower than in 250 μ m channels (Fig. 3d, e). An increased number of large complexes were present in the smaller channels relative to the 250 μ m channel (Fig. 2), which may result from aggregation of the complexes and thus reducing the transfection efficiency [21,22]. The greater surface area in the 250 μ m channels relative to smaller channels may enable complexes to deposit independently. Complexes in the smaller channels presumably aggregate when they deposit adjacent to or on neighboring complexes, which could limit either cellular internalization or trafficking.

Neurons cultured in the 100 μ m PLG channels extended longer primary neurites and exhibited significantly less branching as compared to neurons in larger channels. Primary neurites extend directly from the neuron cell soma and secondary neurites branch from the primary, which is hypothesized to occur in the absence of guidance cues in order to explore the environment [23]. As branching occurs, the growth of a primary neurite slows and is followed by cytoskeleton rearrangement and extension of a secondary growth cone [8]. A higher ratio of primary neurites is desired, as branching results in several shorter neurites, and longer primary neurites are more likely to cross a lesion. Primary neurite extension was greater and branching was minimal in the 100 μ m channel, suggesting a directional cue within the channel. This directional cue may be physical guidance resulting from the channel walls. The closer spacing of the walls in the 100 μ m channel relative to larger channels increases the probability that a neurite will contact the wall and extend parallel to it. Previously, channels 20–30 μ m wide (the same order of magnitude as filopodia) directed neurites down the channel, potentially by limiting the angles at which the microtubules and actin filaments accumulate and assemble within the neurite shaft and growth cone [8].

Transfected accessory cells cultured within channel walls resulted in localized secretion of NGF at the PLG surface. Neurons can extend neurites across micropatterned grooves to span the channel [24]; however, neurites spanning the channel were not observed in this report. Neurotrophic factor expression on the polymer likely maintains the neurites at the surface, and can also facilitate

physical guidance. Furthermore, localized secretion of the therapeutic factor will concentrate the secreted protein and can potentially maintain the protein at a therapeutic level. Neurons cultured in the 100 µm channels exhibited an increase in primary neurite density as compared to the larger channels, which was independent of the NGF concentration (Fig. 5f). Additionally, the extent of this increase in primary neurite density was higher when neurons were co-cultured with pNGF transfected cells as compared to neurons with NGF added to the media. Together, these results suggest that the pNGF transfected cells may also direct extending neurites, in addition to the guidance by the channel walls.

The system presented here may offer specific advantages over previously developed methods to promote and direct neurite extension. Patterning adhesion molecules (e.g., ECM proteins) can guide cellular adhesion and neurite extension [25–27]. A challenge in patterning adhesive proteins or peptides to guide cellular processes *in vivo* is the non-specific adsorption of various proteins present in serum, or proteins deposited by the cells, which can mask or displace the immobilized molecules. Alternatively, physical barriers have been fabricated using a photolithographic technique to pattern polyimide walls with widths ranging from 20 to 60 µm [8]. While the physical barriers with smaller widths provided a more efficient physical guidance, regenerating neurites *in vivo* are likely to grow in bundles, and may require channels on the order of 100 µm in diameter [28]. Importantly, physical barriers or patterned ECM can provide necessary directional cues, but do not maintain therapeutic levels of growth promoting signals, which is a factor limiting regeneration *in vivo*. The developed system provides physical guidance, while simultaneously altering the expression profile of cells cultured in the channels. Gene delivery from tissue engineering scaffolds can alter gene expression for time scales on the order of months [14]. Here, the sustained expression can maintain therapeutic concentrations with transfected cells localized to the PLG in order to provide a path across the lesion.

The immobilization of DNA complexes to the PLG enabled the localization of individual genes at specific channels, which has not been demonstrated to our knowledge and would be challenging using traditional drug delivery methods. The ability to localize protein production to specific regions of a tissue engineering scaffold may facilitate the regeneration of complex tissues, such as the spinal cord. The white matter of the spinal cord contains several distinct tracts, both motor and sensory, that respond differentially to various neurotrophic factors, such as NGF, neurotrophins (NT-3, NT-4/5), glial-derived neurotrophic factor (GDNF), and BDNF [29]. For example, NGF promotes the growth of sensory neurons [30], while combinations of BDNF, GDNF, and NT-3 promote the growth of axons within the corticospinal tract [31]. Tissue engineering strategies for spinal cord regeneration may require that factor delivery be spatially controlled

to target the various axon populations within the spinal cord. In this report, the patterned deposition of DNA complexes produced localized expression of the proteins, with no cells in the EGFP channel expressing DsRed, and vice versa (Fig. 6). The system presented here extends the capabilities of substrate-mediated delivery on patterned PLG, and has implications for tailoring individual channels to recreate the complex architecture of the spinal cord.

5. Conclusions

PLG substrates that promote and direct axonal elongation were developed using topographically patterned PLG and gene delivery. Gene delivery by immobilization to the PLG surface resulted in transfection efficiency and transgene expression dependent upon the channel width and DNA amount. An *in vitro* neuronal co-culture model demonstrated that neurons cultured in smaller width PLG microchannels exhibited a greater degree of directionality and less secondary sprouting than larger channels. Additionally, surface immobilization enabled gene transfer to be localized to specific regions of the polymer, which may facilitate the regeneration of complex tissues. These studies have identified design principles for translation to 3D constructs and *in vivo* nerve regeneration.

Acknowledgments

The authors thank Stoyan Smoukov, Angela Pannier, and Erin West (Northwestern University) for technical assistance with photolithography, microchannel fabrication, and complex pipetting. Photolithography was performed at the Materials Processing and Crystal Growth core facility and confocal images were obtained at the Biological Imaging Facility (Northwestern University). Financial support for this research was provided by grants from NIH (R01 GM066830, LDS) and NSF (Graduate Research Fellowship, THR).

References

- [1] Yiu G, He Z. Glial inhibition of CNS axon regeneration. *Nat Rev Neurosci* 2006;7(8):617–27.
- [2] David S, Lacroix S. Molecular approaches to spinal cord repair. *Annu Rev Neurosci* 2003;26:411–40.
- [3] Geller HM, Fawcett JW. Building a bridge: engineering spinal cord repair. *Exp Neurol* 2002;174(2):125–36.
- [4] Schmidt CE, Leach JB. Neural tissue engineering: strategies for repair and regeneration. *Annu Rev Biomed Eng* 2003;5:293–347.
- [5] Zhang N, Yan H, Wen X. Tissue-engineering approaches for axonal guidance. *Brain Res Rev* 2005;49(1):48–64.
- [6] Yang Y, De Laporte L, Rives CB, Jang JH, Lin WC, Shull KR, et al. Neurotrophin releasing single and multiple lumen nerve conduits. *J Control Release* 2005;104(3):433–46.
- [7] Moore MJ, Friedman JA, Lewellyn EB, Mantila SM, Krych AJ, Ameenuddin S, et al. Multiple-channel scaffolds to promote spinal cord axon regeneration. *Biomaterials* 2006;27(3):419–29.
- [8] Mahoney MJ, Chen RR, Tan J, Saltzman WM. The influence of microchannels on neurite growth and architecture. *Biomaterials* 2005;26(7):771–8.

- [9] Friedman JA, Windebank AJ, Moore MJ, Spinner RJ, Currier BL, Yaszemski MJ. Biodegradable polymer grafts for surgical repair of the injured spinal cord. *Neurosurgery* 2002;51(3):742–51 discussion 51–2.
- [10] Bunge MB. Bridging areas of injury in the spinal cord. *Neuroscientist* 2001;7(4):325–39.
- [11] Bregman BS, Coumans JV, Dai HN, Kuhn PL, Lynskey J, McAtee M, et al. Transplants and neurotrophic factors increase regeneration and recovery of function after spinal cord injury. *Prog Brain Res* 2002; 137:257–73.
- [12] Boyd JG, Gordon T. Neurotrophic factors and their receptors in axonal regeneration and functional recovery after peripheral nerve injury. *Mol Neurobiol* 2003;27(3):277–324.
- [13] Whittlesey KJ, Shea LD. Delivery systems for small molecule drugs, proteins, and DNA: the neuroscience/biomaterial interface. *Exp Neurol* 2004;190(1):1–16.
- [14] Jang JH, Rives CB, Shea LD. Plasmid delivery in vivo from porous tissue-engineering scaffolds: transgene expression and cellular transfection. *Mol Ther* 2005;12(3):475–83.
- [15] Segura T, Volk MJ, Shea LD. Substrate-mediated DNA delivery: role of the cationic polymer structure and extent of modification. *J Control Release* 2003;93(1):69–84.
- [16] Bengali Z, Pannier AK, Segura T, Anderson BC, Jang JH, Mustoe TA, et al. Gene delivery through cell culture substrate adsorbed DNA complexes. *Biotechnol Bioeng* 2005;90(3):290–302.
- [17] Segura T, Shea LD. Surface-tethered DNA complexes for enhanced gene delivery. *Bioconjugate Chem* 2002;13(3):621–9.
- [18] Jang JH, Bengali Z, Houchin TL, Shea LD. Surface adsorption of DNA to tissue engineering scaffolds for efficient gene delivery. *J Biomed Mater Res Part A* 2006;77A(1):50–8.
- [19] Whittlesey KJ, Shea LD. Nerve growth factor expression by PLG-mediated lipofection. *Biomaterials* 2006;27(11):2477–86.
- [20] Meijering E, Jacob M, Sarria JCF, Steiner P, Hirlimann H, Unser M. Design and validation of a tool for neurite tracing and analysis in fluorescence microscopy images. *Cytometry Part A* 2004;58A(2): 167–76.
- [21] Lee H, Jeong JH, Park TG. PEG grafted polylysine with fusogenic peptide for gene delivery: high transfection efficiency with low cytotoxicity. *J Control Release* 2002;79(1–3):283–91.
- [22] Koyama Y, Ito T, Matsumoto H, Tanioka A, Okuda T, Yamaura N, et al. Novel poly(ethylene glycol) derivatives with carboxylic acid pendant groups: synthesis and their protection and enhancing effect on non-viral gene transfection systems. *J Biomater Sci Polym Ed* 2003;14(6):515–31.
- [23] Kalil K, Szebenyi G, Dent EW. Common mechanisms underlying growth cone guidance and axon branching. *J Neurobiol* 2000; 44(2):145–58.
- [24] Goldner JS, Bruder JM, Li G, Gazzola D, Hoffman-Kim D. Neurite bridging across micropatterned grooves. *Biomaterials* 2006;27(3): 460–72.
- [25] Kam L, Shain W, Turner JN, Bizios R. Axonal outgrowth of hippocampal neurons on micro-scale networks of polylysine-conjugated laminin. *Biomaterials* 2001;22(10):1049–54.
- [26] Miller C, Jeftnija S, Mallapragada S. Synergistic effects of physical and chemical guidance cues on neurite alignment and outgrowth on biodegradable polymer substrates. *Tissue Eng* 2002; 8(3):367–78.
- [27] Heller DA, Garga V, Kelleher KJ, Lee TC, Mahbubani S, Sigworth LA, et al. Patterned networks of mouse hippocampal neurons on peptide-coated gold surfaces. *Biomaterials* 2005;26(8):883–9.
- [28] Anderson MJ, Waxman SG. Regeneration of spinal neurons in inframammalian vertebrates: morphological and developmental aspects. *J Hirnforsch* 1983;24(4):371–98.
- [29] Jones LL, Oudega M, Bunge MB, Tuszyński MH. Neurotrophic factors, cellular bridges and gene therapy for spinal cord injury. *J Physiol* 2001;533(Part 1):83–9.
- [30] Ramer MS, Priestley JV, McMahon SB. Functional regeneration of sensory axons into the adult spinal cord. *Nature* 2000;403(6767): 312–6.
- [31] Zhou L, Shine HD. Neurotrophic factors expressed in both cortex and spinal cord induce axonal plasticity after spinal cord injury. *J Neurosci Res* 2003;74(2):221–6.